Development 136, 3669-3678 (2009) doi:10.1242/dev.041954

Progressive interdigital cell death: regulation by the antagonistic interaction between fibroblast growth factor 8 and retinoic acid

Rocío Hernández-Martínez, Susana Castro-Obregón and Luis Covarrubias*

The complete cohort of molecules involved in interdigital cell death (ICD) and their interactions are yet to be defined. Bmp proteins, retinoic acid (RA) and Fgf8 have been previously identified as relevant factors in the control of ICD. Here we determined that downregulation of *Fgf8* expression in the ectoderm overlying the interdigital areas is the event that triggers ICD, whereas RA is the persistent cell death-inducing molecule that acts on the distal mesenchyme by a mechanism involving the induction of *Bax* expression. Inhibition of the mitogen-activated protein kinase (Mapk) pathway prevents the survival effect of Fgf8 on interdigital cells and the accompanying Erk1/2 phosphorylation and induction of *Mkp3* expression. Fgf8 regulates the levels of RA by both decreasing the expression of *Raldh2* and increasing the expression of *Cyp26b1*, whereas RA reduces *Fgfr1* expression and Erk1/2 phosphorylation. In the mouse limb, inhibition of Bmp signaling in the mesenchyme does not affect ICD. However, noggin in the distal ectoderm induces *Fgf8* expression and reduces interdigit regression. In the chick limb, exogenous noggin reduces ICD, but, when applied to the distal mesenchyme, this reduction is associated with an increase in *Fgf8* expression. In agreement with the critical decline in *Fgf8* expression for the activation of ICD, distal interdigital cells acquire a proximal position as interdigit regression occurs. We identified proliferating distal mesenchymal cells as those that give rise to the interdigital cells fated to die. Thus, ICD is determined by the antagonistic regulation of cell death by Fgf8 and RA and occurs through a progressive, rather than massive, cell death mechanism.

KEY WORDS: Limb, Programmed cell death, Apoptosis, Morphogenesis, CD1 Mouse, Chick, Bmp

INTRODUCTION

Interdigital cell death (ICD) is a morphogenetic event associated with digit separation in chick and mouse. The current model supposes the formation of an interdigital tissue that subsequently degenerates and, as a result, digits individualize. Selective growth of digits could also contribute to digit separation. Under this model, ICD would restrict the growth of the interdigital tissue. Several molecules have been identified that participate in the regulation of ICD; however, very little is known about their mechanism of action and how they interact and contribute to trigger ICD.

Members of the bone morphogenetic protein (Bmp) subfamily of Tgfβ growth factors have been shown to be potent cell death inducers (Buckland et al., 1998; Ganan et al., 1996; Macias et al., 1997; Macias et al., 1999; Yokouchi et al., 1996). *Bmp2*, *Bmp4*, *Bmp5* and *Bmp7* are expressed in the autopod of the developing limb, each with a different but overlapping expression pattern (Francis et al., 1994; Geetha-Loganathan et al., 2006; Lyons et al., 1990; Pajni-Underwood et al., 2007; Robert, 2007; Salas-Vidal et al., 2001; Zuzarte-Luis et al., 2004). In the mouse, near the time of ICD initiation, *Bmp2* and *Bmp7* are preferentially expressed in the interdigital areas, whereas *Bmp4* is mostly found in the distal ectoderm (Pajni-Underwood et al., 2007; Salas-Vidal et al., 2001). The ectopic application of Bmp2, Bmp4, Bmp5 or Bmp7 in the interdigital mesenchyme promotes apoptosis in the chick limb and accelerates interdigit regression (Macias et al., 1997; Rodriguez-Leon et al., 1999; Zuzarte-Luis et al., 2004). In agreement with a function for Bmp in ICD, extensive expression of a dominant-negative type I Bmp receptor early in chick limb development reduces ICD and produces soft tissue syndactyly (Zou and Niswander, 1996). Bmp antagonists, such as noggin or gremlin, produce the same effect when ectopically applied to the interdigital mesenchyme (Merino et al., 1999). In the mouse limb, noggin expression in the apical ectoderm also reduces cell death and causes syndactyly (Guha et al., 2002; Wang et al., 2004). More importantly, mice lacking the Bmp receptor *Bmpr1a* or both *Bmp2* and *Bmp4* specifically in the apical ectodermal ridge (AER) show syndactyly (Maatouk et al., 2009; Pajni-Underwood et al., 2007). Therefore, Bmp members could regulate cell death directly in the mesenchyme (e.g. Bmp7) or indirectly through their activity in the apical ectodermal ridge (e.g. Bmp4).

Retinoic acid (RA) is a broad-spectrum cell death inducer. In the mouse limb, an excess of RA causes distal limb truncations, possibly owing to cell death (Alles and Sulik, 1989; Kochhar et al., 1993) and, when applied just before the onset of ICD, accelerates interdigit regression in mouse and chick limbs (Lussier et al., 1993; Rodriguez-Leon et al., 1999). All RA receptor (Rar) genes are expressed in the autopod region of the limb, but only *Rarβ* expression is restricted to the interdigital area (Dollé et al., 1989). Mouse embryos lacking *Rarβ* are viable and show no abnormalities in the limb. However, supporting the role of RA in ICD, $Rar\beta^{-/-}$; $Rar\gamma^{-/-}$ double mutant embryos show interdigital webbing and an absence of interdigital *Bmp7* expression (Dupé et al., 1999). In the chick limb, it has also been proposed that RA is a physiological regulator of ICD as an all-trans-RA receptor antagonist decreases ICD (Rodriguez-Leon et al., 1999).

Several members of the Fgf family play a role in limb development. In particular, limb growth is promoted by the positive-feedback loop between different Fgf members, with Fgf4, Fgf8 and Fgf10 being the most important (Niswander, 2003). Fgf members

Department of Developmental Genetics and Molecular Physiology, Instituto de Biotecnología, Universidad Nacional Autónoma de México, Cuernavaca, Morelos 62210, México.

*Author for correspondence (covs@ibt.unam.mx)

Accepted 2 September 2009

have survival activity in developing limbs as indicated by their ability to reduce ICD when applied ectopically (Macias et al., 1996). This Fgf survival activity could be responsible for the growth-promoting activity of the AER. Fgf8, the gene of which is expressed throughout the AER during limb growth, is likely to be the most important factor performing this function. That endogenous Fgf8 promotes a survival activity in the distal limb mesenchyme is suggested from the syndactyly phenotype and reduction in ICD associated with its persistent expression in several mutant and transgenic mice (Guha et al., 2002; Lallemand et al., 2005; Wang et al., 2004), as well as its restricted expression to the digit tip ectoderm at the time ICD begins (Salas-Vidal et al., 2001).

Complex interactions are likely to occur among the factors participating in the control of ICD. Presently, little information exists regarding the mechanism by which different factors control ICD. Despite the data described above, the expression patterns of *Rarβ*, *Bmp2*, *Bmp4*, *Bmp7*, and the homeobox genes *Msx1* and *Msx2*, in the mouse do not correlate in time and/or space with the ICD pattern (Salas-Vidal et al., 2001). Furthermore, it is known that many of the genes that might participate in ICD have other functions early in limb development. Therefore, evidence supporting a role of these genes in ICD, in which the effect of the experimental treatment is evaluated after other processes have occurred, should be taken with caution. For example, in the mouse, gene-specific deletions causing syndactyly occur long before ICD begins, leaving the possibility that the phenotype is the result of a sum of alterations occurring before ICD (Dupé et al., 1999; Lallemand et al., 2005; Pajni-Underwood et al., 2007).

We hypothesized that *Fgf8* downregulation in the distal interdigital ectoderm triggers ICD. To better define the direct contribution of RA, Bmp7 and Fgf8 in ICD activation, we studied their regulatory function in cell death in a short time window (of no longer than 8 hours). We found that Fgf8 and RA are crucial regulators of ICD, the former preventing, and the latter promoting, cell death. Bmp activity in the mesenchyme, by contrast, appears to be required for ICD in the chick but not for ICD in the mouse. We discuss the participation of these signals in the context of a progressive ICD model of digit individualization.

MATERIALS AND METHODS

Animals

Mouse strain CD1 was used in this study. Pregnant females were sacrificed by cervical dislocation from 12.5 to 13.5 days postcoitus (dpc; day 0.5 of coitus was the day on which a vaginal plug was found). Embryos were selected according to the limb stage required. Fore- or hind-limbs were dissected without preference, but always considering the limb developmental stage. Chick embryos [stage 28-30 (Hamburger and Hamilton, 1992)] were taken from fertilized eggs incubated for 6 to 7 days. The eggs were windowed at the desired stage and the right or left limb was exposed.

Mouse limb culture

The limb culture protocol used here was as previously described (Salas-Vidal et al., 1998). Limbs were staged according to Wanek's system (Wanek et al., 1989). The stage indicated in the figures is that at which the experiment was performed. Solutions of growth factors [1 mg/ml in phosphate buffered saline (PBS)] were used to soak heparin beads (Fgf8, Peprotech; Bmp7, R&D Systems) or Affi-gel beads (noggin, R&D Systems) for 1 hour at room temperature. In the experiments presented, beads with growth factor were always implanted in the D3-D4 interdigital area of mouse limbs. The control beads were incubated in PBS and implanted in the D2-D3 interdigital area. Retinoic acid (10 μM, Sigma), retinoic acid receptor antagonist AGN193109 (100 μM, Allergan), Fgfr antagonist SU5402 (50 μM, Calbiochem), Mapk inhibitor UO126 (50 μM, Calbiochem), phosphoinositide 3-kinase (Pi3k) inhibitor LY294002 (25-50 μM, Calbiochem) and dorsomorphin (15 μM, Calbiochem) were added directly to the culture medium for 6 or 8 hours. For each treatment, at least three independent experiments were performed in triplicate; reproducibility in each condition tested was generally higher than 90%.

Cell death detection

As a common practice, all limbs used in this study were stained with Acridine Orange (AO) in order to ensure the limb stage and/or the effectiveness of the treatments carried out. Lysotracker (LT; Molecular Probes) staining was used to detect dying cells and specific gene expression in the same sample. The TUNEL Kit (Roche) assay was used to detect apoptotic cells in 7-10 μm sections of paraffin-embedded tissues. The complete series was analyzed by confocal fluorescence microscopy. To detect cell death in developing chick limbs, they were rinsed in a Neutral Red solution (1 mg/ml in PBS) for 10 minutes at room temperature, then washed in PBS for 5 minutes, and finally viewed by fluorescence microscopy.

Wholemount in situ hybridization and immunodetection

Wholemount in situ hybridization was performed as previously described (Salas-Vidal et al., 2001). Riboprobes were synthesized using the DIG RNA Labeling Kit (Roche) according to the manufacturer's recommendations. Probes for the following genes were used: *Fgf8*, *Bmp7*, *Mkp3* (also known as *Dusp6*), *Msx2*, *Raldh2* (*Aldh1a2*–Mouse Genome Informatics), *Cyp26b1*, *Bcl2*, *Bclx* and *Bax*. Immunohistochemistry in wholemount was performed as previously described (Corson et al., 2003). Primary antibodies used were phospho-Erk1/2 (pErk1/2), phospho-Smad1/5/8 (pSmad), Smad1, cleaved caspase 3 (all from Cell Signaling Technology) and Fgf8 (Sigma). After incubation with a biotinylated anti-rabbit secondary antibody (Vector Laboratories), the signal was developed with the Vectastain HRP-Avidin-Biotin Complex (ABC) Reagent (Vector Laboratories).

Adenoviral infection

Small drops (20 μl) of supernatant from cultures of cells producing Ad-EGFP or Ad-noggin-EGFP adenovirus were placed on parafilm within a humidified chamber. Stage 8 (S8) mouse limbs were dissected, placed in the small drops with the adenovirus and incubated for 2 hours in a 5% CO_2 incubator. After adenovirus infection, mouse limbs were cultured on 0.45 μm durapore filters (Millipore) floating on DMEM (Invitrogen) with 10% fetal bovine serum and without antibiotic supplementation for up to 48 hours. Three independent experiments performed in triplicate with the same infection efficiency were analyzed.

BrdU incorporation

Mouse limbs before ICD initiation (S8-S9) were immersed in a 10 μmol/l BrdU/DMEM solution (Roche) and incubated at 37°C in a 5% CO_2 incubator for 1 hour. Right limbs were fixed immediately in 4% paraformaldehyde overnight, whereas left limbs were first washed in 3 ml dissection medium (L15; Microlab) and then cultivated for 12 hours as described above, before fixing. After TUNEL labeling, BrdU incorporation was detected by first incubating samples in 4 M HCl for 20 minutes (for antigen retrieval), followed by neutralization with 0.1 M boric acid, three washes in PBS, and a 2-hour incubation with anti-BrdU Alexa-Fluor 594 (Molecular Probes) in PBS. After one further wash in PBS, the complete series was analyzed by confocal fluorescence microscopy.

RESULTS

Cell death fate of distal interdigital cells

We previously estimated the growth of digital and interdigital regions around the time ICD occurs by comparison of digitalized limb contours (Salas-Vidal et al., 2001); however, the actual origin of the dying interdigital tissue has not been determined. We inserted a bead into the distal mesenchyme of both chick and mouse limbs just before the start of ICD. As shown in Fig. 1A, a significant amount of mouse interdigital tissue developed above the bead, indicating that interdigits grow within a 12-hour time window. In the chick, a significant proportion of the interdigital tissue also originated by growth after ICD began (Fig. 1B).

These previous results suggest that all dying interdigital cells derive from the most distal proliferating cells. In order to test this, distal interdigital cells were labeled with BrdU and their fate was followed during the formation of the dying interdigital region. One hour after BrdU addition, labeled cells were found all along a distal margin defining a 100 μm region (Fig. 1C). Twelve hours later, most BrdU-labeled cells were dying (92.5±9%; n=4) and were located in a more proximal region (Fig. 1C). Therefore, distal cells initiate the death process as they progressively acquire a lateral and proximal position.

Fgf8 downregulation triggers ICD in the mouse

Fgf8 is expressed in the distal ectoderm around the time that ICD and digit individualization initiate (Salas-Vidal et al., 2001); thus, distal proliferating cells are likely to be under the influence of this growth factor. Consistent with previous work showing that Fgf2 and Fgf4 have survival activity on interdigital mesenchymal cells (Macias et al., 1996), we observed that Fgf8-soaked beads implanted in the interdigital regions of S8-S9 mouse limbs, stages just prior to, or coincident with, the initiation of ICD, decreased ICD as determined by AO staining or TUNEL (Fig. 2A). Interestingly, application of the Fgf8 bead after ICD initiation (S9-S10) only slightly affected cell death (data not shown).

If Fgf8 is relevant for the survival of distal mesenchymal cells, downregulation of its gene could be the direct cause of ICD. An analysis of *Fgf8* expression and cell death in the same limb along several developmental stages around the initiation of ICD supports this possibility (Fig. 3). In S8 limbs, *Fgf8* expression was detected in the entire distal ectoderm without evidence of ICD. In limbs at a later stage than S8 but before S9 (S8+), *Fgf8* expression decreased in the interdigital ectoderm, and cell death was initiated in the underlying mesenchyme. Finally, in S9 limbs, *Fgf8* expression was restricted to the digital apical ectoderm and cell death extended laterally and proximally into the interdigital mesenchyme regions. Fgf8 and activated caspase 3 (an indicator of dying cells) showed the same pattern (data not shown).

In order to determine whether Fgf signaling contributes to the survival of distal mesenchyme, we studied the consequences of inhibiting Fgf receptor (Fgfr) tyrosine kinase activity in S8 limbs. Fgfr inhibition promoted cell death in the distal mesenchyme (Fig. 2B). In S9-S10 limbs, Fgfr inhibition increased cell death at the tips of digits, a location coincident with the mesenchyme underneath the Fgf8-expressing ectoderm (data not shown). Taking these data together, Fgf8 appears to be a survival factor in the distal mesenchyme of limbs around the time that digits individualize, and its disappearance could be the direct cause of the onset of ICD.

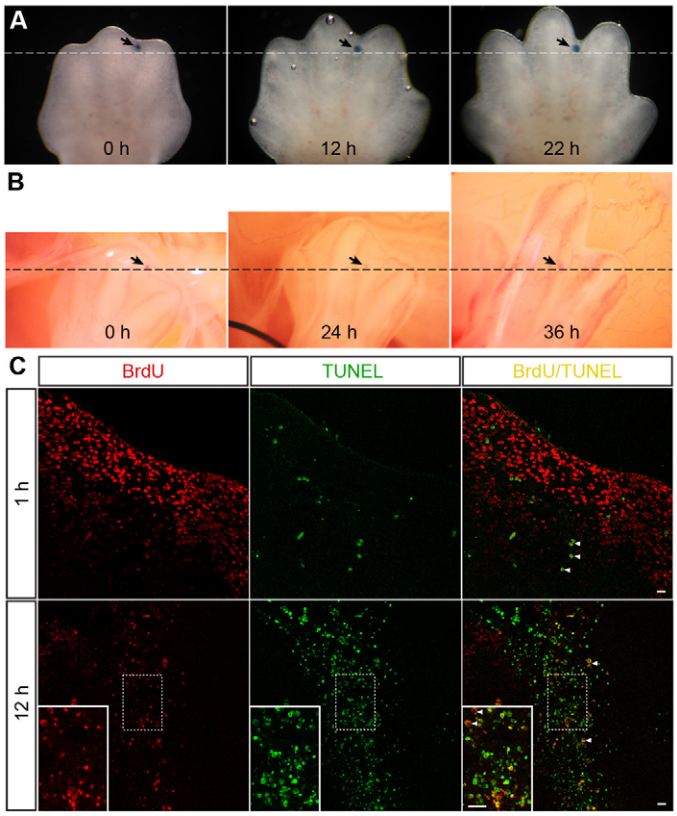

Fig. 1. Fate of distal mesenchymal cells of interdigital zones. (**A**) A bead was implanted in the distal region of mouse S8 limbs just at the time interdigital cell death (ICD) begins (0 hours). The bead was used as a reference (dashed line) to follow the growth and regression of the interdigital tissue at later times during ICD in the same limb in culture. Note that, 12 hours after ICD initiated, there was small but significant growth of the interdigital tissue. This tissue regressed 10 hours later as digital areas continued growing. (**B**) As in A, but chick limbs in ovo were used. The bead was implanted into limbs of stage-28 embryos around the time ICD initiates. The same limbs with the implanted bead were followed for up to 36 hours. As in the mouse, there was an initial growth of the interdigital areas, which then stopped growing as digital zones projected distally. (**C**) Distal proliferating mesenchymal cells of mouse limbs were labeled by culturing limbs for 1 hour in the presence of BrdU (red). Limbs were cultured for a further 12 hours in the absence of BrdU, and the cell death fate determined by TUNEL (green). Note that almost all interdigital BrdU-labelled cells died. Arrowheads indicate autofluorescent erythrocytes. Scale bar: 20 μm.

The Mapk pathway mediates the Fgf8 survival effect

In the limb bud, Fgf8 can signal using the classical Ras-Mapk pathway (Delfini et al., 2005; Eblaghie et al., 2003; Echevarria et al., 2005). Accordingly, phosphorylation of the Mapk member Erk1/2 is closely associated with the AER Fgf8 activity during limb bud growth (Corson et al., 2003). The expression of *Mkp3* (encoding a Mapk phosphatase) is also associated with this activity, suggesting that a negative-feedback loop regulates Fgf8/Mapk signaling (Eblaghie et al., 2003; Echevarria et al., 2005; Li et al., 2007). Nevertheless, it has been shown that the Pi3k pathway mediates the Fgf8 survival effect and activation of *Mkp3* expression during growth of chick limb buds (Kawakami et al., 2003). In concordance with the lack of participation of Pi3k in the Fgf8 survival activity, the Pi3k inhibitor LY294002 did not affect the *Mkp3* expression pattern in the distal mesenchyme of S8 or S9 limbs (see Fig. S1A,B in the supplementary material). Furthermore, the survival effect of exogenous Fgf8 was clearly not altered by the Pi3k inhibitor, and under these circumstances *Mkp3* expression was markedly upregulated compared with that of untreated limbs (see Fig. S1B in the supplementary material).

In contrast to the previous results, in the presence of U0126 [a Mapk (Mek) inhibitor], cell death in S8 limbs was expanded proximally (Fig. 4A) and the protective effect of Fgf8 on the interdigital cells of S9 limbs was suppressed (Fig. 4B). Consistent with an effect reducing survival activity, Mek inhibition increased the number of TUNEL-positive cells (Fig. 4B). In agreement with a marked reduction in Fgf8 activity, the Mek inhibitor completely blocked *Mkp3* expression induced by both endogenous Fgf8 produced in the distal ectoderm of S8 limbs (Fig. 4A) and exogenous

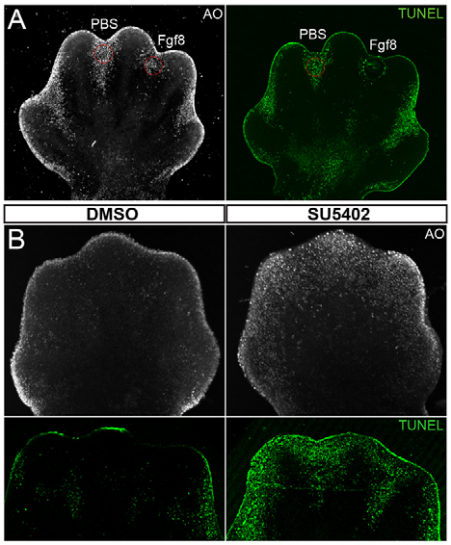

Fig. 2. Fgf8 survival activity in the interdigital mesenchyme. (**A**) S9 mouse limbs were treated for 8 hours with an Fgf8-soaked bead or a bead soaked in PBS (control). Fgf8 treatment greatly reduced the number of dying cells [Acridine Orange (AO) or TUNEL] in the interdigital regions. (**B**) S8 mouse limbs were treated with DMSO (control) or SU5402 (an Fgf receptor inhibitor) for 8 hours. Note that SU5402 increased distal cell death (AO or TUNEL).

Fgf8 implanted in the interdigits of S9 limbs (Fig. 4B). As expected from the above results, Erk1/2 was found phosphorylated in the mesenchyme near to the Fgf8 source, either in a naturally occurring state (i.e. distal ectoderm; Fig. 4A) or exogenously added (Fig. 4B), and the Mek inhibitor blocked such phosphorylation (Fig. 4A,B). These data suggest that, at least around the time that ICD begins, the survival effect of Fgf8 on mesenchymal cells is mediated by the Mapk pathway.

Retinoic acid induces cell death in the mouse limb

Although evidence indicates that RA is a positive regulator of ICD (Dupé et al., 1999; Lussier et al., 1993; Rodriguez-Leon et al., 1999), it is unclear whether only interdigital cells are responsive to this molecule, or whether this is a broader property of limb mesenchymal cells. Mouse limbs cultured with RA showed signs of cell death after 3 hours of treatment (data not shown), although induction of cell death was more evident between 6 and 8 hours of treatment. RA induced cell death in the entire distal mesenchyme of S8 limbs (Fig. 5A; also see Fig. S2 in the supplementary material). In S9 mouse limbs, at which stage ICD had already begun, RA increased the ongoing cell death and also induced cell death at the tip of the digits (Fig. 5B; also see Fig. S2 in the supplementary material). Endogenous RA showed the same death-inducing activity, as ICD decreased when S9 limbs were cultured with a Rar antagonist (AGN193109; Fig. 5C; also see Fig. S2 in the supplementary material). Therefore, all distal mesenchymal cells are responsive to the death-inducing activity of RA, suggesting that, in the presence of RA, a survival activity is needed to allow growth. Furthermore, these data support the view that, as in the chick, RA is a direct physiological regulator of ICD in the mouse limb.

The pro-apoptotic Bcl2 family members Bax and Bak appear to play a role in the activation of ICD (Lindsten et al., 2000). Therefore, it is possible that RA controls the expression of their corresponding genes. A bioinformatical approach detected, within 1.5 kb upstream of the transcription initiation sites, three putative RA-responsive elements in *Bax* and one in *Bak* (see Table S1 in the supplementary material). Before ICD initiates, *Bax* is expressed along the whole distal mesenchyme (Fig. 5D). In agreement with a role of RA in the regulation of *Bax* expression in the developing limb, *Bax* mRNA was upregulated by RA and downregulated by a Rar antagonist (Fig. 5D,E).

Retinoic acid and Fgf8 are antagonistic regulators of ICD

Taking the previous data together, it is possible that Fgf8 provides the survival activity that counteracts the death-inducing activity of RA, and thus this antagonism could modulate ICD activation. Indeed, as shown in Fig. 6A, Fgf8 reduced RA-induced cell death. The protection level provided by Fgf8 was RA dose dependent (data not shown), suggesting that the balance between these two signals defines the fate of distal mesenchymal cells.

Fgf8 might prevent RA-induced cell death by decreasing the RA concentration. In vivo, the concentration of RA is regulated by a balance between its synthesis and inactivation. Raldh2 is responsible for most of the RA-synthesizing activity during early mouse embryogenesis (Niederreither et al., 1999). By contrast, members of the Cyp26 family specifically metabolize RA to an inactive form (Fujii et al., 1997). An Fgf8-soaked bead in the interdigital region caused downregulation of *Raldh2* expression,

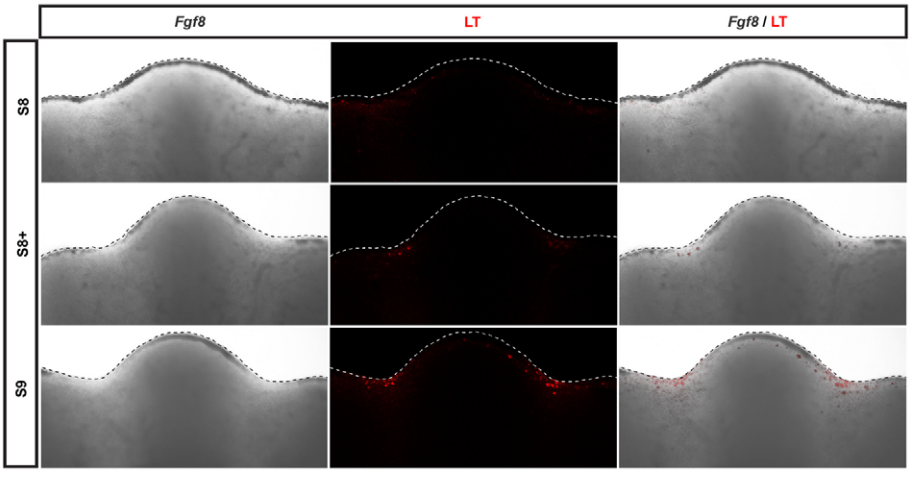

Fig. 3. *Fgf8* expression at the initiation of ICD. Whole limbs at different developmental stages around the time of initiation of ICD (S8-S9), previously stained with Lysotracker (LT; red), were hybridized with an Fgf8 probe. After hybridization, images from the same limb, one showing the distribution of dying cells (LT staining pattern) and the other the *Fgf8* expression pattern (dark signal at the distal ectoderm), were superimposed. ICD was detectable at stages later than S8 (S8+, S9), when *Fgf8* expression began to restrict to the digital ectoderm.

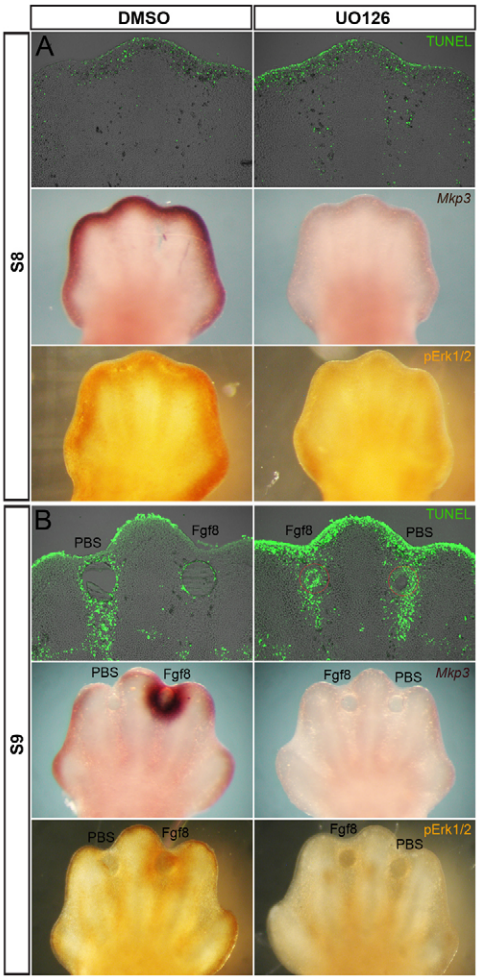

Fig. 4. Effect of Mapk pathway inhibition on *Mkp3* expression and cell death. (**A**) S8 and (**B**) S9 limbs were cultured in the absence (DMSO) or presence of a Mapk kinase inhibitor (UO126, a Mek inhibitor) for 8 hours. S9 limbs carried an Fgf8-soaked bead in the D3-D4 interdigit. In S8 limbs, Mek inhibition increased the number of TUNEL-positive cells in the mesenchyme underlying the distal ectoderm. In S9 limbs, Mek inhibition also increased TUNEL-positive cells, which were particularly evident at the tips of digits. Mek inhibition blocked the survival effect of exogenous Fgf8, as reduction in TUNEL detection was not observed in the presence of the inhibitor. Notably, *Mkp3* expression and Erk phosphorylation were abolished by Mek inhibition, including that induced by exogenous Fgf8.

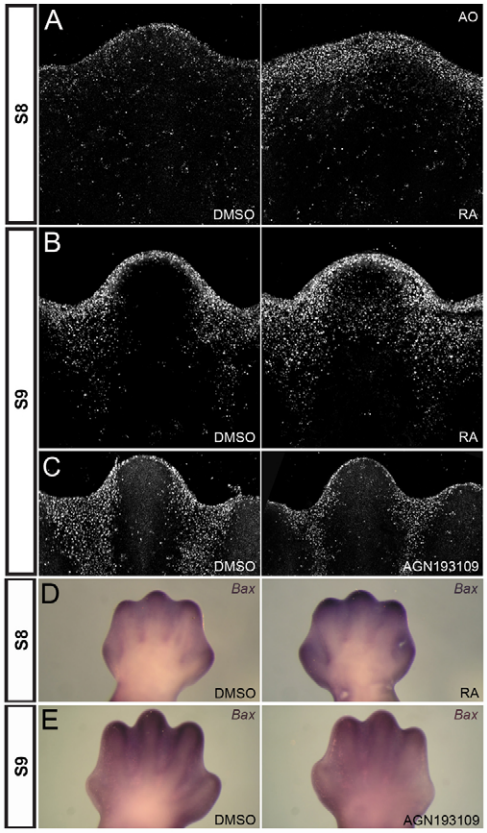

Fig. 5. Activation of cell death by RA in distal and interdigital mesenchyme. (**A-E**) Limbs at two developmental stages, before (S8; A), and at the time of ICD activation (S9; B), were cultured for 8 hours in the absence (DMSO) of RA and a Rar inhibitor, the presence of RA or the presence of a Rar inhibitor (AGN193109; C). After culture, whole limbs were stained with AO (A-C) or limb sections processed for TUNEL detection (see Fig. S2 in the supplementary material). In addition, *Bax* expression was determined by in situ hybridization (D,E). Exogenous RA was a strong cell death inducer in the distal mesenchyme of S8 mouse limbs and in the interdigital mesenchyme and the tips of the digits of S9 limbs. By contrast, physiological ICD in S9 limbs decreased with inhibition of Rar. *Bax* was preferentially expressed in the distal mesenchyme. This expression increased in S8 limbs treated with RA and was reduced in S9 limbs treated with the Rar antagonist.

which was evident after 8 hours of treatment (Fig. 6B). By contrast, the Fgf8-soaked bead upregulated the expression of *Cyp26b1*, which encodes the major enzyme located in the mesenchyme (Fig. 6C). Although RA alone upregulated *Cyp26b1* expression, it was further increased by Fgf8 (see Fig. S2 in the supplementary material). These data indicate that Fgf8 protects from RA-induced cell death by reducing RA production and increasing RA inactivation.

We also evaluated whether RA induces cell death by regulating the expression of *Fgf8* and *Fgfr1*. *Fgfr1* is expressed primarily in the mesenchyme of the developing mouse limb and appears responsible for most Fgf8 activity (Li et al., 2005; Verheyden et al., 2005). Under conditions in which RA increased cell death, *Fgf8* expression did not change (Fig. 6D), but the expression of *Fgfr1* significantly decreased (Fig. 6E). Accordingly, RA exogenously added to cultures of S8 and S9 limbs reduced Erk1/2 phosphorylation caused by endogenous Fgf8 (Fig. 6F). Therefore, RA could provoke cell death, at least partially, by regulating Fgf8 intracellular signaling in distal mesenchymal cells.

As RA upregulated *Bax* expression, we determined whether Fgf8 could counteract the death-inducing activity of RA by controlling the expression or activity of anti-apoptotic Bcl2 members. RA downregulated *Bcl2* expression, but the expression pattern did not suggest a function in ICD (see Fig. S3 in the supplementary material). By contrast, the anti-apoptotic *BclxL* (*Bcl2l1* – Mouse Genome Informatics) was also expressed in the limb (see Fig. S3A in the supplementary material); however, we could not detect regulation by either RA or Fgf8 (data not shown).

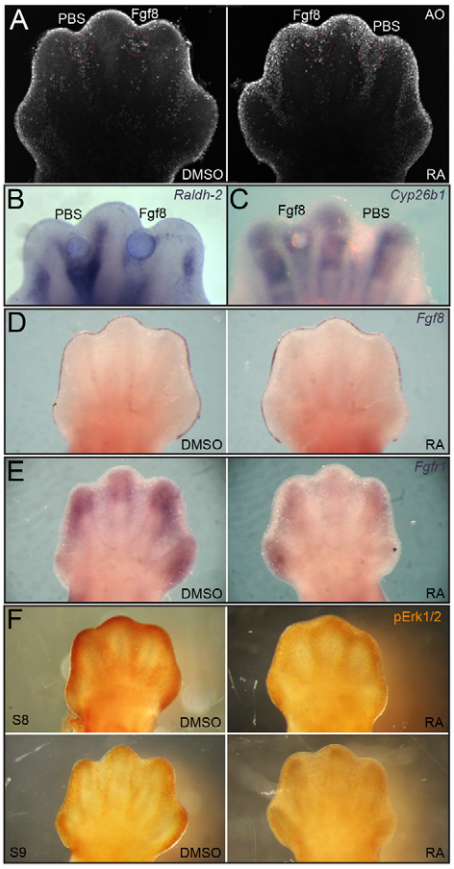

Fig. 6. Antagonistic regulation between Fgf8 and RA signaling. (**A-F**) S8 or S9 limbs were cultured for 8 hours in the absence (DMSO) or presence of RA (A,D-F). In some cases, an Fgf8-soaked bead was implanted in the D3-D4 interdigit (A-C). Fgf8 prevented not only the normal ICD, but also the cell death induced by exogenous RA (A; AO). In the presence of exogenous Fgf8, *Raldh2* expression in the interdigital mesenchyme was downregulated (B), whereas *Cyp26b1* expression was upregulated (C). Conversely, RA had no effect on *Fgf8* expression (D), but downregulated *Fgfr1* expression (E). RA also caused a reduction in Erk phosphorylation in S8 (distal mesenchyme) and in S9 (mesenchyme in the tips of digits) limbs after 4 hours of treatment (F).

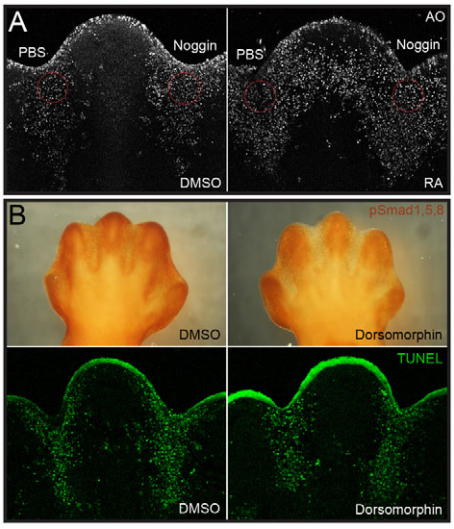

Fig. 7. Mesenchymal Bmp function in the activation of ICD in the mouse limb. S9 limbs were cultured for 8 hours under different conditions. (**A**) A noggin-soaked bead was implanted in the D3-D4 interdigit of S9 limbs in the absence (DMSO) or presence of RA in the culture medium. (**B**) S9 limbs were also cultured in the absence (DMSO) or presence of dorsomorphin, an inhibitor of Smad phosphorylation. Note that no effect on cell death (AO or TUNEL) was detected after inhibiting Bmp activity. A decrease in Smad phosphorylation is indicative of the effect of dorsomorphin on Bmp activity.

Bmp7 function in ICD

At the time that ICD begins, the only Bmp expressed in the interdigital regions of mouse limbs is *Bmp7*, whereas *Bmp4* expression is predominant in the distal ectoderm (Pajni-Underwood et al., 2007; Salas-Vidal et al., 2001). We found that *Bmp7* expression in the mouse limb was regulated by RA and Fgf8, and Bmp7 induced cell death in the distal mesenchyme and negatively regulated *Fgf8* expression in the ectoderm (see Fig. S4 in the supplementary material). Surprisingly, a noggin-soaked bead in the interdigital region did not decrease cell death after 12 hours of culture (starting at S8-S9) or in the presence of RA (Fig. 7A), although noggin did efficiently inhibit cell death induced by exogenous Bmp7 (data not shown). Furthermore, the same noggin-soaked beads in the chick limb decreased ICD after 8 hours of treatment, with an increasing effect up to 24 hours. Noggin inhibited cell death in both the distal (Fig. 8A) and proximal (Fig. 8B) mesenchyme. Interestingly, *Fgf8* expression persisted in the AER when noggin prevented distal ICD (Fig. 8A), but not when it prevented proximal ICD (Fig. 8B). Therefore, Bmp7 (or another Bmp with the ability to bind noggin) in the mesenchyme participates in ICD activation in the chick but not in the mouse limb.

To confirm that mesenchymal Bmp members do not participate in ICD in the mouse limb, we inhibited Smad activity with dorsomorphin, a recently identified compound that prevents Smad phosphorylation (Yu et al., 2008). Dorsomorphin markedly reduced Smad phosphorylation in the interdigital areas of S9 limbs after 8 hours of treatment (Fig. 7B). Reduction was also observed in distal digital areas, although it was less apparent. This might be due to the high levels of Smad1 in digits (R.H.-M. and L.C., unpublished) or the less efficient inhibitory effect of dorsomorphin on Smad1. Despite the reduction in phosphorylated Smad (pSmad) in the presence of dorsomorphin, ICD was not affected (Fig. 7B).

Our previous data contrast with the results observed in transgenic mice that overexpress noggin, in which interdigital regression is reduced, thus suggesting a participation of Bmp members (Guha et al., 2002; Wang et al., 2004). However, in those studies, noggin was overexpressed in the ectoderm; therefore, we hypothesized that modulation of ICD by Bmp proteins is limited to the ectoderm where it regulates *Fgf8* expression. To test this idea, we infected the ectoderm of S8 limbs with an adenovirus that carries noggin coding sequences and EGFP. Twenty-four hours after infection, we observed that *Fgf8* expression in the interdigital ectoderm of infected areas was persistent and both cell death and indentation at the interdigits was reduced in comparison with control limbs infected with an adenovirus carrying only EGFP (Fig. 9A,C). Interdigital webbing generated by noggin-expressing adenovirus increased at 48 hours after infection (data not shown). Similar results were observed when dorsomorphin was applied to S8 limbs (Fig. 9B,C). The marked reduction in cell death observed in these experiments (Fig. 9B)

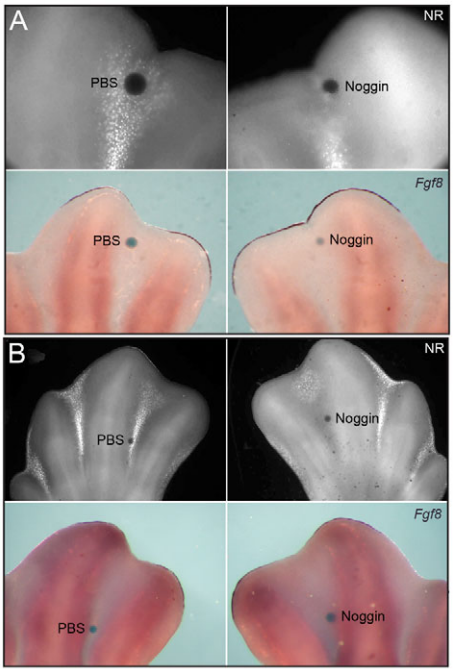

Fig. 8. Bmp activity in the control of ICD in the chick limb. Noggin- or Fgf8 (PBS controls)-soaked beads were implanted in the interdigital region of limbs of stage-28 chick embryos. Noggin was implanted in the (**A**) distal or (**B**) proximal region of the interdigits. Twelve hours later, limbs were stained with neutral red (NR), followed by the determination of *Fgf8* expression. Noggin was able to reduce cell death in the distal or proximal region, but prevention of the normal downregulation of *Fgf8* expression was only observed when noggin was applied distally.

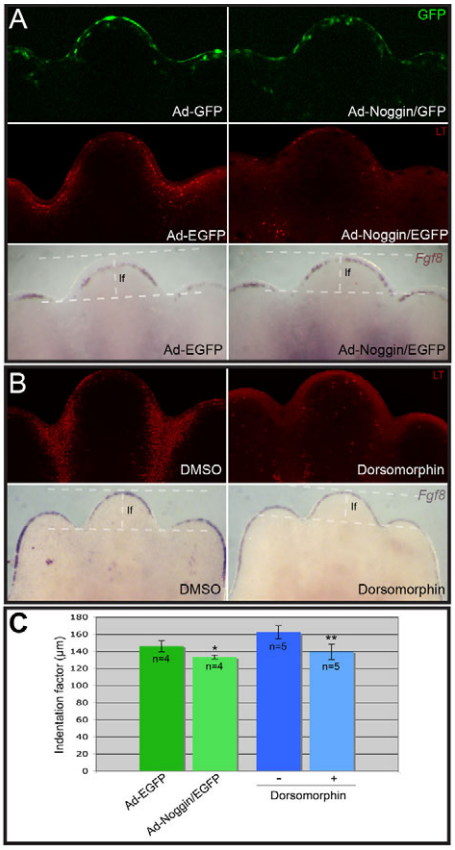

Fig. 9. Ectodermal Bmp function in the activation of ICD in the mouse limb. (**A**) S8 limbs were infected with either an adenovirus carrying the EGFP gene (expression seen in green) alone (Ad-EGFP) or fused to noggin (Ad-noggin/EGFP) and then cultured for 24 hours. (**B**) Alternatively, S8 limbs were treated with dorsomorphin for 12 hours. In limbs infected with Ad-noggin/EGFP or treated with dorsomorphin, some *Fgf8* expression persisted in distal ectoderm. Note the evident reduction in cell death (LT) after treatment of S8 limbs with dorsomorphin or infected with Ad-noggin/EGFP. (**C**) The level of indentation was estimated by determining the 'indentation factor' (IF, labeled as If). IF is the distance between the line touching the lower part of the adjacent interdigits and the parallel line touching the most distal part of the digit in between. Bars are the average ±s.d. IF for the samples indicated. Note that IF was reduced in the interdigital regions of samples infected with Ad-noggin/EGFP (*, $P<0.01$) or treated with dorsomorphin (**, $P<0.005$).

contrasts with the above-described data showing that dorsomorphin, at stages later than S8, was incapable of reducing cell death, and suggest that Bmp acts upstream of *Fgf8* downregulation.

DISCUSSION

The present work proposes a mechanism by which ICD is activated. Our findings suggest that downregulation of *Fgf8* expression is the trigger of ICD and that RA is the essential cell death inducer. Interestingly, Bmp members in the mouse interdigital mesenchyme are not essential for ICD activation, and only an ectodermal Bmp, probably Bmp2 and/or Bmp4 (Maatouk et al., 2009), appears to be required. Our data suggest that an antagonistic interaction between Fgf8 and RA is the major mechanism that controls ICD in the mouse and also contributes to ICD regulation in the chick (Fig. 10A). This mechanism, together with the origin of the interdigital tissue fated to die, support a new model of how ICD contributes to limb morphogenesis (Fig. 10B).

Bmp role in ICD

The requirement of Bmp members in ICD has been determined by three strategies: (1) overexpression of dominant-negative forms of Bmpr (Pizette and Niswander, 1999); (2) adding Bmp antagonists such as noggin and gremlin (Guha et al., 2002; Merino et al., 1999; Wang et al., 2004); and (3) mutations in Bmp or Bmpr genes (Bandyopadhyay et al., 2006; Pajni-Underwood et al., 2007). Nonetheless, in most of these studies, the spatial and/or temporal requirement of Bmp activity for ICD was not determined. The most common view is that Bmp members act directly on mesenchymal cells of interdigits; however, recent studies in which *Bmpr1a* or *Bmp2*/*Bmp4* were specifically inactivated in the AER suggest that AER Bmp activity can indirectly regulate ICD (Bandyopadhyay et al., 2006; Pajni-Underwood et al., 2007). Our data support this latter view in which Bmp activity causes the *Fgf8* downregulation observed in the ectoderm overlying the interdigital tissue. However, it is important to consider that *Fgf8* could also have, in addition to a role in survival, a mitogenic activity on mesenchymal cells; thus, the persistence of Fgf8 might have a double effect that promotes the interdigital tissue growth.

In the mouse limb, we did not find evidence supporting a direct role of Bmp in ICD. Application of noggin in the interdigital mesenchyme did not prevent ICD, even after 24 hours of culture (data not shown). Furthermore, blocking Smad phosphorylation with dorsomorphin in

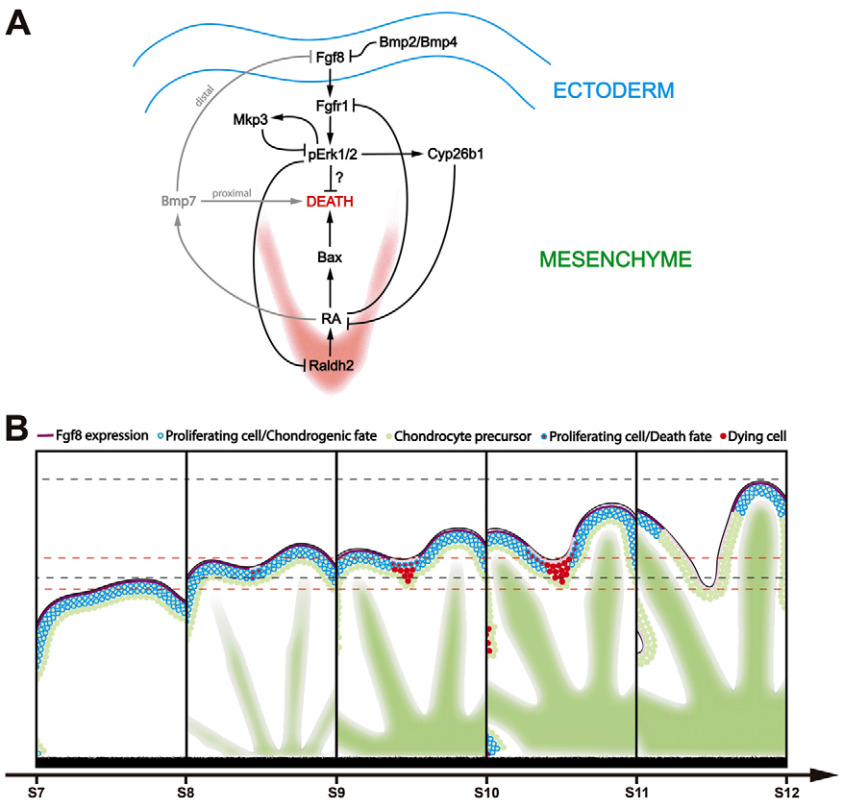

Fig. 10. Molecular and cellular models of the ICD process. (**A**) Antagonistic interaction between Fgf8 and RA at the onset of ICD. RA in this model is the persistent death signal acting continuously on the distal limb mesenchyme, whereas Fgf8 is the survival factor required to promote distal growth. Fgf8 keeps the RA levels low and supports the survival of the growing distal mesenchyme by activating the Mapk pathway. As the limb reaches the stage at which ICD begins, *Fgf8* expression is downregulated, possibly owing to an increase in Bmp activity within the interdigital distal ectoderm, and consequently RA levels increase. RA antagonizes the Mapk survival pathway by reducing the levels of *Fgfr1* expression and phosphorylated Erk1/2 levels, and activates *Bax* expression. In the chick, mesenchymal Bmp7 also negatively regulates *Fgf8* expression, triggering distal ICD, but its role in the control of proximal ICD is Fgf8 independent. (**B**) Progressive ICD. Contrary to the idea that ICD occurs on a preformed tissue, we propose that ICD occurs progressively as the limb grows, allowing the distal projection of digits. After *Fgf8* downregulation (dark to light purple), proliferating interdigital cells are fated to die, whereas the surviving digital cells follow the chondrogenic fate. Black and red dashed lines are references to visualize digital and interdigital growth, respectively.

S9 limbs produced the same result. Bmp also does not mediate ectopic cell death induced by RA, as the expression pattern of Bmp7, the main candidate to play a role in ICD in the mouse, did not correlate with the observed pattern of cell death (see Fig. S4A in the supplementary material), and noggin did not affect the increase in cell death. Furthermore, expression of *Msx2*, which has been considered the end effector for Bmp-mediated apoptosis (Marazzi et al., 1997; Rodriguez-Leon et al., 1999), is downregulated at the beginning of ICD and is strongly induced by ectopic Fgf8 in the interdigits of both mouse and chick limbs in association with the survival activity (see Fig. S5 in the supplementary material). In the chick, our data support the Bmp role in ICD suggested in previous reports but also suggest the possibility that Bmp plays different roles in distal and proximal ICD. Bmp might induce distal ICD by downregulating *Fgf8* expression in the distal ectoderm, whereas induction of proximal ICD by Bmp does not appear to affect *Fgf8* expression. In the mouse, ICD activation appears to be similar to the distal ICD proposed for the chick. Indeed, it has been observed that ICD in the chick begins from distal and proximal regions, whereas in the mouse, proximal ICD is scarcely detected (Fernandez-Teran et al., 2006). It is possible that the large interdigital region in the chick requires different mechanisms to activate ICD in order to completely separate the digits.

RA role in ICD

In the limb, the distal region is the most sensitive to the RA death effects (Alles and Sulik, 1989). Our data show that, at around the time interdigital regression occurs, all distal mesenchyme is competent to die by RA. This competence is associated with the expression of several genes encoding RA receptors, such as *Rarg, Rarg* and *Rxra* (Dollé et al., 1989). It is interesting to note that the domain of *Rarb* expression in the limb that was the first indication of a possible role of RA in ICD is not within the competence region observed at early stages (Dollé et al., 1989; Salas-Vidal et al., 2001). However, the *Rarb*; *Rarg* double mutant has the most penetrant syndactyly phenotype (Dupé et al., 1999). Accordingly, the antagonistic inhibition of Rarα or Rarβ does not affect ICD in the time window studied here (R.H.-M. and L.C., unpublished), suggesting that Rarγ might be the essential active receptor promoting cell death. At this time, with the information available, an indirect interaction between *Rarb* and *Rarg* cannot be discounted.

In agreement with previous reports (Dupé et al., 1999; Rodriguez-Leon et al., 1999), our data indicate that RA is essential for ICD. However, these reports propose that RA activates cell death indirectly by upregulating *Bmp7* (mouse and chick) and *Bmp4* (chick) expression. Our data do not support this possibility in the mouse, as RA activated cell death in regions in which *Bmp7* expression was not induced and noggin did not reduce RA-induced cell death. We propose that RA activates cell death directly without the intervention of Bmp members. In the medial epithelial seam of the developing palate, which also expresses *Bmp4* and *Bmp7*, the cell-death-inducing activity of RA is also Bmp independent (Cuervo et al., 2002). In agreement with this proposal, we show that RA positively regulates the expression of the pro-apotic gene *Bax*. Distal mesenchyme *Bax* (and likely also *Bak*) expression is at least in part controlled by RA, supporting the idea that a survival factor is required to counteract the persistent RA-induced death activity. Our data suggest that Fgf8 is this survival factor, the effects of which are also regulated by RA.

Regulation of Fgf8 survival activity in the control of ICD onset

Although previous reports indicate that Fgf members are survival factors for mesenchymal cells of the developing limb, they do not indicate how this survival activity contributes to the initiation of ICD. We confirmed that Fgf8 has survival activity on mouse

interdigital mesenchyme cells, but more importantly, we showed that *Fgf8* expression is downregulated at the time ICD begins. In agreement with a role of endogenous Fgf8 in interdigital cell survival, several conditions that reduce ICD and cause syndactyly are associated with preserving *Fgf8* expression in the ectoderm overlying the interdigital areas. For instance, reduction in Bmp activity by both noggin protein (Guha et al., 2002; Wang et al., 2004) and *Bmpr1a*- or *Bmp2*/*Bmp4*-specific knockout in ectoderm (Pajni-Underwood et al., 2007) prevents the normal downregulation of *Fgf8* expression in the interdigital distal ectoderm. Similarly, the $Msx1^{-/-}$; $Msx2^{-/-}$ double mutant retains *Fgf8* expression in interdigital distal ectoderm (Lallemand et al., 2005). Supporting the idea that *Fgf8* expression is the direct cause of the lack of ICD and syndactyly in previous reports, constitutive *Fgf4* expression in the distal ectoderm was found to cause syndactyly (Lu and Martin, 2006). Our data, and a study in the chick (Ganan et al., 1998) showing that Bmp7-induced cell death is associated with downregulation of *Fgf8* expression, are also in concordance with the crucial role of Fgf8 for survival of distal interdigital mesenchyme.

Fgf8 survival activity appears to be mediated by two mechanisms (Fig. 10A). Our data suggest that Fgf8 indirectly prevents cell death by decreasing RA synthesis and increasing its inactivation, which results in a global reduction in RA levels. During limb development, RA diffuses from proximal to distal regions. At around the time ICD begins, RA is synthesized in the proximal region of the interdigits [defined by *Raldh2* expression (Niederreither et al., 1999)], and diffuses to the distal area where Fgf8 presumably reduces RA levels by increasing the amount of Cyp26b1. In vivo, induction of *Cyp26b1* expression in the presence of Fgf8 is apparent when ICD begins and *Cyp26b1* expression restricts to the digits. Antagonistic regulation between Fgf8 and RA appears to be a common mechanism in the control of developmental processes (Abu-Abed et al., 2001; Diez del Corral et al., 2003; Mercader et al., 2000).

Our data suggest that Fgf8 also promotes its survival activity by a direct mechanism through the Mapk pathway. This conclusion comes from the evident requirement of Mek activity for the Fgf survival activity and the direct association of this activity with Erk1/2 phosphorylation and *Mkp3* expression. Given that RA activates *Bax* expression, the end target of this signaling pathway might be anti-apoptotic Bcl2 members. Bcl2 and BclxL do not appear to be good candidates, but more members and post-translational modifications need to be studied in order to define whether this is a plausible antagonistic mechanism controlling ICD. On the other hand, RA has no perceptible effect on *Fgf8* expression but does promote a reduction in *Fgfr1* expression. In addition, RA negatively regulates Erk1/2 phosphorylation by a mechanism apparently independent of upregulation of *Mkp3* expression. Therefore, RA might also be able to antagonize Fgf8 survival activity and, in this way, promote cell death.

Massive versus progressive ICD

The areas with phosphorylated Erk and *Mkp3* expression define the domain of action of Fgf8 survival activity. This domain does not cover the whole interdigital area, suggesting that proximal ICD is triggered by a different mechanism. Our model proposes that most interdigital cells derive from the distal mesenchyme, the survival of which depends on Fgf8. Thus, all cells that die in the interdigital region must be at some point within the domain of Fgf8 action (estimated as no more than 100 μm of the underlying mesenchyme based on the zone of proliferating cells). Interestingly, our data with mouse limbs show that the interdigital tissue, defined as the region with abundant cell death before digit individualization, is generated within a 12 hour time window after the initial detection of dying cells. Proximal dying cells in the interdigital mesenchyme included those cells that were underlying the distal ectoderm at the time ICD began. As is the case with digits, interdigits also grow but distal projection is restricted by cell death. According to this view, cell death is initiated in the distal region, and, as the limb grows, dying cells acquire a proximal position (Fig. 10B). Our model proposes that ICD in the mouse, rather than being a process of massive cell death, is mostly a progressive mechanism. In the chick, distal ICD might use the same mechanism described above for the mouse limb, but the most proximal ICD appears to follow a different mechanism that is dependent on interdigital Bmp activity.

Acknowledgements

We thank Ivor Mason, Brigid Hogan, Pierre Chambon, Juan Carlos Ispizúa-Belmonte, Benoit Robert and Arturo Álvarez-Buylla for kindly providing the mouse Fgf8, Bmp, RA receptors, Mkp3 cDNA clones, Msx genomic fragment clones and the Ad-noggin-GFP, respectively; Jesús Chimal-Monroy for his generosity in providing the chick eggs used in this study; Concepción Valencia, Elizabeth Mata, Sergio González, Marcela Ramírez and Andrés Saralegui for their technical assistance; and Christopher Wood for careful reading of the manuscript. This work was supported by grant IN218607 from PAPIIT-DGAPA.

Supplementary material

Supplementary material for this article is available at
http://dev.biologists.org/cgi/content/full/136/21/3669/DC1

References

Abu-Abed, S., Dolle, P., Metzger, D., Beckett, B., Chambon, P. and Petkovich, M. (2001). The retinoic acid-metabolizing enzyme, CYP26A1, is essential for normal hindbrain patterning, vertebral identity, and development of posterior structures. *Genes Dev.* **15**, 226-240.

Alles, A. J. and Sulik, K. K. (1989). Retinoic-acid-induced limb-reduction defects: perturbation of zones of programmed cell death as a pathogenetic mechanism. *Teratology* **40**, 163-171.

Bandyopadhyay, A., Tsuji, K., Cox, K., Harfe, B. D., Rosen, V. and Tabin, C. J. (2006). Genetic analysis of the roles of BMP2, BMP4, and BMP7 in limb patterning and skeletogenesis. *PLoS Genet.* **2**, e216.

Buckland, R. A., Collinson, J. M., Graham, E., Davidson, D. R. and Hill, R. E. (1998). Antagonistic effects of FGF4 on BMP induction of apoptosis and chondrogenesis in the chick limb bud. *Mech. Dev.* **71**, 143-150.

Corson, L. B., Yamanaka, Y., Lai, K. M. and Rossant, J. (2003). Spatial and temporal patterns of ERK signaling during mouse embryogenesis. *Development* **130**, 4527-4537.

Cuervo, R., Valencia, C., Chandraratna, R. A. and Covarrubias, L. (2002). Programmed cell death is required for palate shelf fusion and is regulated by retinoic acid. *Dev. Biol.* **245**, 145-156.

Delfini, M. C., Dubrulle, J., Malapert, P., Chal, J. and Pourquie, O. (2005). Control of the segmentation process by graded MAPK/ERK activation in the chick embryo. *Proc. Natl. Acad. Sci. USA* **102**, 11343-11348.

Diez del Corral, R., Olivera-Martinez, I., Goriely, A., Gale, E., Maden, M. and Storey, K. (2003). Opposing FGF and retinoid pathways control ventral neural pattern, neuronal differentiation, and segmentation during body axis extension. *Neuron* **40**, 65-79.

Dolle, P., Ruberte, E., Kastner, P., Petkovich, M., Stoner, C. M., Gudas, L. J. and Chambon, P. (1989). Differential expression of genes encoding alpha, beta and gamma retinoic acid receptors and CRABP in the developing limbs of the mouse. *Nature* **342**, 702-705.

Dupé, V., Ghyselinck, N. B., Thomazy, V., Nagy, L., Davies, P. J. A., Chambon, P. and Mark, M. (1999). Essential roles of retinoic acid signaling in interdigital apoptosis and control of BMP-7 expression in mouse autopods. *Dev. Biol.* **208**, 30-43.

Eblaghie, M. C., Lunn, J. S., Dickinson, R. J., Munsterberg, A. E., Sanz-Ezquerro, J. J., Farrell, E. R., Mathers, J., Keyse, S. M., Storey, K. and Tickle, C. (2003). Negative feedback regulation of FGF signaling levels by Pyst1/MKP3 in chick embryos. *Curr. Biol.* **13**, 1009-1018.

Echevarria, D., Martinez, S., Marques, S., Lucas-Teixeira, V. and Belo, J. A. (2005). Mkp3 is a negative feedback modulator of Fgf8 signaling in the mammalian isthmic organizer. *Dev. Biol.* **277**, 114-128.

Fernandez-Teran, M. A., Hinchliffe, J. R. and Ros, M. A. (2006). Birth and death of cells in limb development: a mapping study. *Dev. Dyn.* **235**, 2521-2537.

Francis, P. H., Richardson, M. K., Brickell, P. M. and Tickle, C. (1994). Bone morphogenetic proteins and a signalling pathway that controls patterning in the developing chick limb. *Development* **120**, 209-218.

Fujii, H., Sato, T., Kaneko, S., Gotoh, O., Fujii-Kuriyama, Y., Osawa, K., Kato, S. and Hamada, H. (1997). Metabolic inactivation of retinoic acid by a novel

P450 differentially expressed in developing mouse embryos. *EMBO J.* **16**, 4163-4173.
Ganan, Y., Macias, D., Duterque-Coquillaud, M., Ros, M. A. and Hurle, J. M. (1996). Role of TGF betas and BMPs as signals controlling the position of the digits and the areas of interdigital cell death in the developing chick limb autopod. *Development* **122**, 2349-2357.
Ganan, Y., Macias, D., Basco, R. D., Merino, R. and Hurle, J. M. (1998). Morphological diversity of the avian foot is related with the pattern of msx gene expression in the developing autopod. *Dev. Biol.* **196**, 33-41.
Geetha-Loganathan, P., Nimmagadda, S., Huang, R., Scaal, M. and Christ, B. (2006). Expression pattern of BMPs during chick limb development. *Anat. Embryol. (Berl.)* **211 Suppl. 1**, 87-93.
Guha, U., Gomes, W. A., Kobayashi, T., Pestell, R. G. and Kessler, J. A. (2002). In vivo evidence that BMP signaling is necessary for apoptosis in the mouse limb. *Dev. Biol.* **249**, 108-120.
Hamburger, V. and Hamilton, H. L. (1992). A series of normal stages in the development of the chick embryo. 1951. *Dev. Dyn.* **195**, 231-272.
Kawakami, Y., Rodriguez-Leon, J., Koth, C. M., Buscher, D., Itoh, T., Raya, A., Ng, J. K., Esteban, C. R., Takahashi, S., Henrique, D. et al. (2003). MKP3 mediates the cellular response to FGF8 signalling in the vertebrate limb. *Nat. Cell Biol.* **5**, 513-519.
Kochhar, D. M., Jiang, H., Harnish, D. C. and Soprano, D. R. (1993). Evidence that retinoic acid-induced apoptosis in the mouse limb bud core mesenchymal cells is gene-mediated. *Prog. Clin. Biol. Res.* **383B**, 815-825.
Lallemand, Y., Nicola, M. A., Ramos, C., Bach, A., Cloment, C. S. and Robert, B. (2005). Analysis of Msx1; Msx2 double mutants reveals multiple roles for Msx genes in limb development. *Development* **132**, 3003-3014.
Li, C., Xu, X., Nelson, D. K., Williams, T., Kuehn, M. R. and Deng, C. X. (2005). FGFR1 function at the earliest stages of mouse limb development plays an indispensable role in subsequent autopod morphogenesis. *Development* **132**, 4755-4764.
Li, C., Scott, D. A., Hatch, E., Tian, X. and Mansour, S. L. (2007). Dusp6 (Mkp3) is a negative feedback regulator of FGF-stimulated ERK signaling during mouse development. *Development* **134**, 167-176.
Lindsten, T., Ross, A. J., King, A., Zong, W. X., Rathmell, J. C., Shiels, H. A., Ulrich, E., Waymire, K. G., Mahar, P., Frauwirth, K. et al. (2000). The combined functions of proapoptotic Bcl-2 family members bak and bax are essential for normal development of multiple tissues. *Mol. Cell* **6**, 1389-1399.
Lu, P., Minowada, G. and Martin, G. R. (2006). Increasing Fgf4 expression in the mouse limb bud causes polysyndactyly and rescues the skeletal defects that result from loss of Fgf8 function. *Development* **133**, 33-42.
Lussier, M., Canoun, C., Ma, C., Sank, A. and Shuler, C. (1993). Interdigital soft tissue separation induced by retinoic acid in mouse limbs cultured in vitro. *Int. J. Dev. Biol.* **37**, 555-564.
Lyons, K. M., Pelton, R. W. and Hogan, B. L. (1990). Organogenesis and pattern formation in the mouse: RNA distribution patterns suggest a role for bone morphogenetic protein-2A (BMP-2A). *Development* **109**, 833-844.
Maatouk, D. M., Choi, K. S., Bouldin, C. M. and Harfe, B. D. (2009). In the limb AER Bmp2 and Bmp4 are required for dorsal-ventral patterning and interdigital cell death but not limb outgrowth. *Dev. Biol.* **327**, 516-523.
Macias, D., Ganan, Y., Ros, M. A. and Hurle, J. M. (1996). In vivo inhibition of programmed cell death by local administration of FGF-2 and FGF-4 in the interdigital areas of the embryonic chick leg bud. *Anat. Embryol. (Berl.)* **193**, 533-541.
Macias, D., Ganan, Y., Sampath, T. K., Piedra, M. E., Ros, M. A. and Hurle, J. M. (1997). Role of BMP-2 and OP-1 (BMP-7) in programmed cell death and skeletogenesis during chick limb development. *Development* **124**, 1109-1117.
Macias, D., Ganan, Y., Rodriguez-Leon, J., Merino, R. and Hurle, J. M. (1999). Regulation by members of the transforming growth factor beta superfamily of the digital and interdigital fates of the autopodial limb mesoderm. *Cell Tissue Res.* **296**, 95-102.
Marazzi, G., Wang, Y. and Sassoon, D. (1997). Msx2 is a transcriptional regulator in the BMP4-mediated programmed cell death pathway. *Dev. Biol.* **186**, 127-138.
Mercader, N., Leonardo, E., Piedra, M. E., Martinez, A. C., Ros, M. A. and Torres, M. (2000). Opposing RA and FGF signals control proximodistal vertebrate limb development through regulation of Meis genes. *Development* **127**, 3961-3970.
Merino, R., Rodriguez-Leon, J., Macias, D., Ganan, Y., Economides, A. N. and Hurle, J. M. (1999). The BMP antagonist Gremlin regulates outgrowth, chondrogenesis and programmed cell death in the developing limb. *Development* **126**, 5515-5522.
Niederreither, K., Subbarayan, V., Dollé, P. and Chambon, P. (1999). Embryonic retinoic acid synthesis is essential for early mouse post-implantation development. *Nat. Genet.* **21**, 444-448.
Niswander, L. (2003). Pattern formation: old models out on a limb. *Nat. Rev. Genet.* **4**, 133-143.
Pajni-Underwood, S., Wilson, C. P., Elder, C., Mishina, Y. and Lewandoski, M. (2007). BMP signals control limb bud interdigital programmed cell death by regulating FGF signaling. *Development* **134**, 2359-2368.
Pizette, S. and Niswander, L. (1999). BMPs negatively regulate structure and function of the limb apical ectodermal ridge. *Development* **126**, 883-894.
Robert, B. (2007). Bone morphogenetic protein signaling in limb outgrowth and patterning. *Dev. Growth Differ.* **49**, 455-468.
Rodriguez-Leon, J., Merino, R., Macias, D., Ganan, Y., Santesteban, E. and Hurle, J. M. (1999). Retinoic acid regulates programmed cell death through BMP signalling. *Nat. Cell Biol.* **1**, 125-126.
Salas-Vidal, E., Lomelí, H., Castro-Obregón, S., Cuervo, R., Escalante-Alcalde, D. and Covarrubias, L. (1998). Reactive oxygen species participate in the control of mouse embryonic cell death. *Exp. Cell Res.* **238**, 136-147.
Salas-Vidal, E., Valencia, C. and Covarrubias, L. (2001). Differential tissue growth and patterns of cell death in mouse limb autopod morphogenesis. *Dev. Dyn.* **220**, 295-306.
Verheyden, J. M., Lewandoski, M., Deng, C., Harfe, B. D. and Sun, X. (2005). Conditional inactivation of Fgfr1 in mouse defines its role in limb bud establishment, outgrowth and digit patterning. *Development* **132**, 4235-4245.
Wanek, N., Muneoka, K., Holler-Dinsmore, G., Burton, R. and Bryant, S. V. (1989). A staging system for mouse limb development. *J. Exp. Zool.* **249**, 41-49.
Wang, C. K., Omi, M., Ferrari, D., Cheng, H. C., Lizarraga, G., Chin, H. J., Upholt, W. B., Dealy, C. N. and Kosher, R. A. (2004). Function of BMPs in the apical ectoderm of the developing mouse limb. *Dev. Biol.* **269**, 109-122.
Yokouchi, Y., Sakiyama, J., Kameda, T., Iba, H., Suzuki, A., Ueno, N. and Kuroiwa, A. (1996). BMP-2/-4 mediate programmed cell death in chicken limb buds. *Development* **122**, 3725-3734.
Yu, P. B., Hong, C. C., Sachidanandan, C., Babitt, J. L., Deng, D. Y., Hoyng, S. A., Lin, H. Y., Bloch, K. D. and Peterson, R. T. (2008). Dorsomorphin inhibits BMP signals required for embryogenesis and iron metabolism. *Nat. Chem. Biol.* **4**, 33-41.
Zou, H. and Niswander, L. (1996). Requirement for BMP signaling in interdigital apoptosis and scale formation. *Science* **272**, 738-741.
Zuzarte-Luis, V., Montero, J. A., Rodriguez-Leon, J., Merino, R., Rodriguez-Rey, J. C. and Hurle, J. M. (2004). A new role for BMP5 during limb development acting through the synergic activation of Smad and MAPK pathways. *Dev. Biol.* **272**, 39-52.